Multiple Damage Types on Carbon Steel and Silica Glass during Ultrasonic Cavitation Erosion

Mengru Fu (1st Author)
Ocean College, Zhejiang University
Hangzhou, China
fumengru@zju.edu.cn

Han Ge (Corresponding Author)
Ocean College, Zhejiang University
Hangzhou, China
gehan@zju.edu.cn

***Abstract*—After 15 min ultrasonic cavitation, the cavitation damages on mild carbon steel (Q235) and silica glass were distinguished from each other due to their different physical properties and failure modes. Q235 steel usually suffered plastic deformation under cavitation and had distinctively distributed pits on the surface due to its good toughness, which looked like craters with sunken center and raised smooth margin. While the damage on silica glass surface was irregular with sharp edges, which was resulted from the good hardness and brittle property of glass. The cavitation erosion of silica glass began with nano scaled cavities, and expanded through cracks on the free surface around cavities, then finally ended with large-area collapse of material. Additionally, simplified numerical models have been calculated to discuss the formative factor of multiple damage types.**

Keywords—cavitation damage; Q235 steel; silica glass; failure mode; COMSOL

I. INTRODUCTION

The rapid alteration of underwater pressure in high-rate flow areas may lead to cavitation [1]. This common event is generally responsible for the occurrence of micro damages or cavitation erosion, which usually appears on treated surfaces of repeated application and causes an undesirable reduction of the lifetime of engine components dealing with fluids involved for industrial or engineering applications (ships propellers, pumps, valves, turbines, nozzles, etc.) [2, 3]. Metallic materials (steel or metal alloys), Non-metallic materials (polymer materials or glasses) with different physical properties or structures have usually been used in the manufacture of hydraulic components because of their different performance advantages.

However, all these materials have to suffer from damage in multiple types due to mechanical impaction during cavitation erosion. Chen et al. had found three kinds of erosion pits (e.g. complete, incomplete and thermal pits) on 40Cr steel surface and explained their formations by the simulation of a bubble collapse process [4]. What's more, they had also investigated the brittle fractures appeared on the medium carbon steel surface at the incubation stage of cavitation erosion [5]. While Matthieu et al. analyzed the phenomena and mechanisms of acoustic cavitation erosion on two glasses, soda lime and fused silica, and pointed out that the correlation between chemical durability and erosion resistance was not obvious [3]. So although numerous researches about cavitation erosion on different material surface have been done, the formative factors of different erosion types on materials remain uncertainty.

Here, in this work, the cavitation erosion characters of two typical materials, e.g. ductile material: mild carbon steel (Q235) and brittle material: silica glass (SiO_2), were analyzed by scanning electron microscope (SEM), metallographic microscope. Also, a numerical method was adopted to further investigate the formative factors of these different damages.

II. EXPERIMENTAL SCHEMATICS

The experiments of cavitation erosion on mild carbon steel and silica glass samples were performed in an ultrasonic vibration system, as shown in Fig. 1. The horn with a diameter of 15 mm vibrated axially in a frequency of 20 kHz and amplitude of ± 6 μm. The samples were mounted on the install table facing the tip of the vibration

978-0-933957-43-5 ©2015 MTS

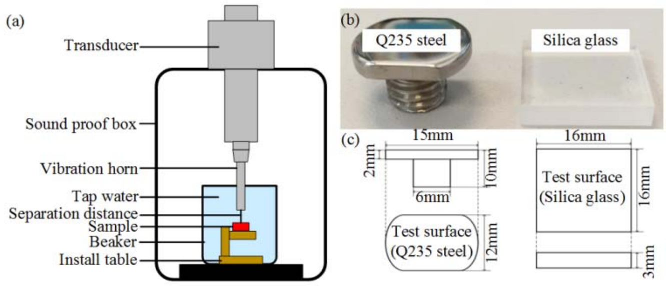

Fig. 1. Experimental setup and samples: (a) ultrasonic cavitation system; (b) samples; (c) sample sizes.

horn at a certain separation distance of 5 mm.

The carbon steel (Q235) and silica glass surfaces were polished respectively to a surface roughness (*R*a) of 36.67 nm ± 10 nm and 1.62 nm ± 1 nm, which was tested by an optical profiler (Wyko NT9100). The properties of these two materials were shown in Table 1. During the experiment, cavitation bubbles, whose collapses near a solid surface can cause cavitation erosion, were generated at the tip surface of vibration horn and directly moved toward the surface of the samples. After 15 min, the samples were taken out to clean and dry. Thereafter, the damages were observed under scanning electron microscope (SEM, FEI-FEG650) and metallographic microscope (ZEISS-Axio Imager A2m).

III. NUMERICAL MODEL

According to some references, an ultrasonic cavitation bubble with a maximum radius of 50 μm usually generated a micro-jet with a diameter of 10 μm [6, 7]. So in this model, the impact of the micro-jet was simplified as an instantaneous load, just like Fig. 2(a) shows. Also, considering the time hysteresis effect from periphery to center caused by the round head of micro-jet [8], the load area was divided into five sections (P_1-P_5, as displayed in Fig. 2(b)) uniformly to add the same impact load in different times.

The impact load was given by the well-known Water Hammer Pressure $P_{WH} = \rho_L \cdot c_L \cdot v_{jet}$ [9] and the Bemoulli

TABLE I. LIST OF MATERIAL PROPERTIES

Property (Unit)	Material	
	Carbon steel (Q235)	*Silica glass*
Density (kg/m^3)	7858	2203
Young's modulus (GPa)	200	66.13
Poisson's ratio	0.25	0.17
Initial yield stress (MPa)	235	—
Isotropic tangent modulus (MPa)	6100	—

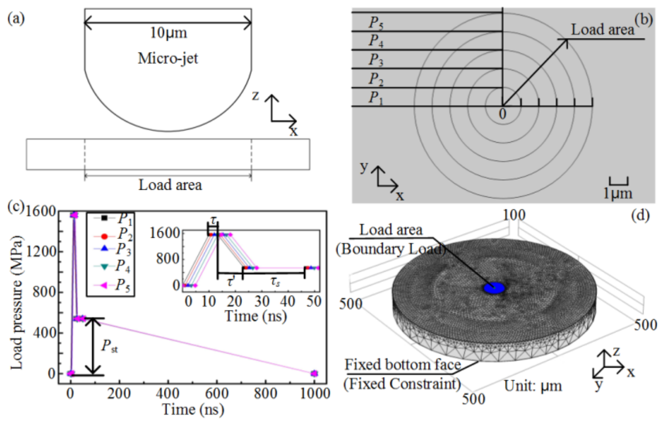

Fig. 2. Simplified numerical model: (a) schematic diagram of micro-jet impact; (b) detailed view of impact area; (c) impact load curves; (d) sample mesh.

Stagnation Pressure $P_{st} = (\rho_L \cdot v_{jet}^2)/2$ [10], where v_{jet} is the striking velocity of jet (here v_{jet} was set as 1040 m/s [11-14]), ρ_L is the density of liquid and c_L is the sound speed in liquid. What's more, the duration τ of Water Hammer Pressure, the time τ' for Water Hammer Pressure to attenuate to the Bemoulli Stagnation Pressure, and the duration τ_s of Bemoulli Stagnation Pressure, could be evaluated by $\tau = d/2c_L$, $\tau' = 3d/2c_L$ [15] and $\tau_s = 2\tau' + \tau$ [16], where d is the diameter of jet. Then, the load curves were derived in Fig. 2(c) and used to simulate the striking process of micro-jet on sample surface in the software COMSOL Multiphysics. The sample in the model was simplified as a thin cylinder to reduce calculation and meshed into a total element number of 53, 326, as shown in Fig. 2(d), and its bottom face was fixed without any rotation or translation to consistent with the experimental condition. Additionally, the time step was set as 1 ns for the first 52 ns, and increased to 50 ns after that.

IV. RESULTS AND DISCUSSIONS

A. Cavitation Erosion on Carbon Steel Surface

Fig. 3 shows the surface profiles of carbon steel after cavitation under metallographic microscope and SEM. The colorful and even overlapping circles, which actually called erosion pits and iridescent rings on Fig. 3(a) indicated that the cavitation erosion experiment was success. A detailed view of erosion pit and iridescent ring was shown in Fig. 3(b) and (c).

The carbon steel used in this experiment was Q235, an elastic-plastic metal. This material would experience two deforming stages when it suffered an increased impact within a short time, as shown in Fig. 4, which gave the numerical results about the formation process of an erosion pit on steel surface. The elastic deformation was the main type in the first deforming stage (from Fig. 4(a) to Fig. 4(b)), and then plastic deformation occurred when the impact load was higher than the material's yield stress (Fig. 4(c)). In the process of cavitation, the impact load of micro-jet induced by bubble collapsing was far more than steel's yield stress. When it struck on metal surface, the micro crystal structure of material in impact area would badly crack and shift in an instant [5]. However, because of the steel's good toughness, the central material had to be pushed to peripheral region instead of peeling off. That's why the pits distributed distinctively and looked like craters with sunken center and raised smooth margin (Fig. 3(b) and Fig. 3(c)).

Moreover, the nanometer particles found around erosion pit in Fig. 3(b) indicated that the impact area had suffered an instantaneous very high temperature during cavitation damage, which led to the melt but rapid crystallization of surrounding metal [17]. Additionally, the heat damage of steel could also be proved by the iridescent ring in Fig. 3(c). The ring is the production of high-temperature oxidation on steel [18], which differed from the damage types of other materials under cavitation erosion.

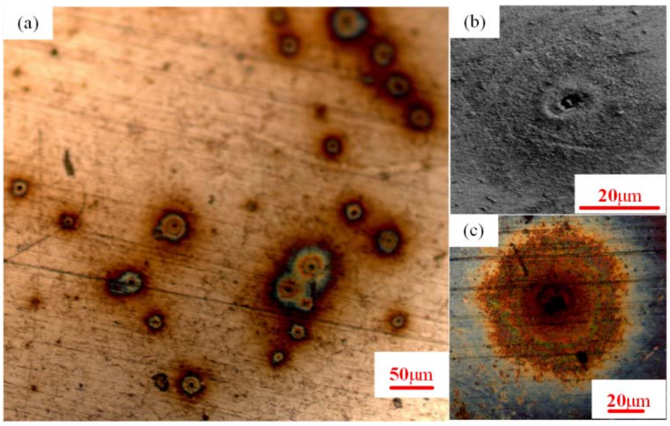

Fig. 3. Surface profiles of Q235 steel after cavitation: (a) Whole view of damages under metallographic microscope; (b) erosion pit under SEM; (c) iridescent ring area around a pit.

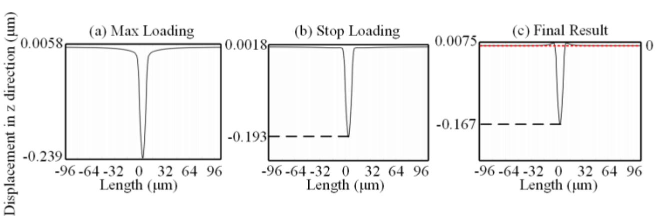

Fig. 4. Numerical results about the formation process of erosion pit on Q235 steel surface.

B. *Cavitation Erosion on Silica Glass Surface*

Compared with Q235 steel, silica glass was much easier to be damaged in cavitation because of its good hardness but poor toughness, which contributed to a high brittleness index (hardness/toughness) [3]. High brittleness index usually leads to a transformation of damage types from ductile to brittle. While the common feature of brittle damage was the stripping of material and expanding irregular cracks, which could explain that it is easy for silica glass to generated nano scaled cavities under the impact of cavitation micro-jet, as shown in Fig. 5(a). These cavities were combined through irregular cracks and expanded to break a certain area [19]. It can be found in Fig. 5(b) that the shape of damage on silica glass was irregular with sharp edges and the free surface around the damage area was serious affected by generating cracks. Finally, the glass surface collapsed in large scale (Fig. 5(c)), and its surface roughness decreased (Fig. 5(a)), which would lead to more serious cavitation erosion. Additionally, a numerical simulation about the formation of a cavity at the initial stage of cavitation damage on silica glass surface was also carried out in Fig. 6. A little elastic deformation of silica glass could be observed due to its slight elastic characteristic, while the formed pit in the final result was so shallow that an enlarged picture had shown the details. The raised part around the pit

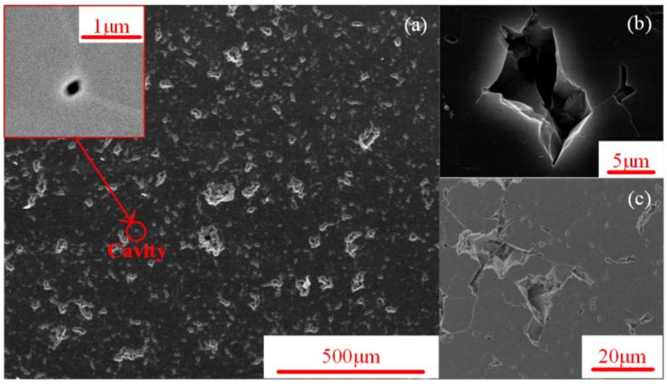

Fig. 5. SEM photos for surface profiles of silica glass after cavitation: (a) Whole view of cavitation damages, a cavity is enlarged in red box; (b) detailed view of local damage; (c) surface collapse.

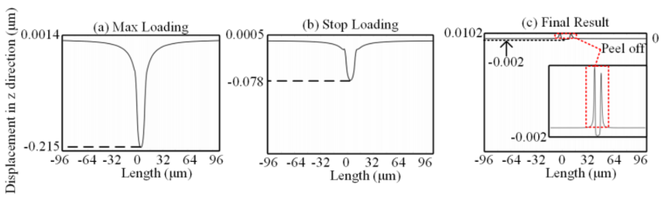

Fig. 6. Numerical results about the formation process of damage on silica glass surface (the raised part in red dotted box would peel off in real damage process).

in final result presented by the red dotted box would peel off in the real damage process, which meant the formation of a cavity.

V. CONCLUSION

Ultrasonic cavitation experiments and corresponding numerical methods have been carried out on the surface of mild carbon steel (Q235) and silica glass. The results distinguished the damage types of the tested materials and revealed that the formative factor was due to the failure modes of materials with different physical properties under transient and enormous local load. For steel, the pits distributed distinctively and looked like craters with sunken center and raised smooth margin, which was due to the good toughness of steel and plastic deformation during cavitation erosion. While, the irregular damage with sharp edges on silica glass began with nano scaled cavities, and expanded through cracks on the free surface around cavities, then finally ended with large-area collapse of material. This damage type was results from the good hardness and brittle character of glass. An understanding of the damage types and mechanism in the typical materials will help facilitate the development of metallic or non-metallic materials able to resist cavitation erosion in many potential applications.

ACKNOWLEDGEMENT

Project (grant no. N20110201) supported by Foundation of Zhejiang Educational Committee, project (grant no. LQ13E050001) supported by Zhejiang Provincial Natural Science Foundation of China and project (grant no. 51405432) supported by NSFC are thanked.

REFERENCES

[1] M. Dular, O.C. Delgosha and M. Petkovsek, "Observations of cavitation erosion pit formation," Ultrason. Sonochem, vol. 20, pp. 1113-1120, July 2013.

[2] J. Lu, K.H. Zum and J. Schneider, "Microstructural effects on the resistance to cavitation erosion of ZrO2 ceramics in water," Wear, vol. 265, pp. 1680–1686, 2008.

[3] Matthieu, C. Tony, I.N. Sergey, G.S. Dmitry, Z. Thomas and M. Helmuth, "Acoustic cavitation at the water-glass interface," J. Phys. Chem. C, vol. 114, pp. 13083-13091, June 2010.

[4] H.S. Chen, J. Li, D.R. Chen and J.D, Wang, "Damages on steel surface at the incubation stage of the vibration cavitation erosion in water," Wear, vol. 265, pp. 692-698, February 2008.

[5] H.S. Chen and S.H. Liu, "Inelastic damages by stress wave on steel surface at the incubation stage of vibration cavitation erosion," Wear, vol. 266, pp. 69-75, July 2009.

[6] Y. Tomita and A. Shima, "Mechanisms of impulsive pressure generation and damage pit formation by bubble collapse," J. Fluid Mech, vol. 169, pp. 535-564, August 1986.

[7] S.G. Lambrakos and N.E. Tran, "Inverse analysis of cavitation impact phenomena on structures," J. Mater. Eng. Perform, vol. 17, pp. 202-209, July 2008.

[8] J. Luo, "Study on cavitation erosion behavior and ultrasonic cavitation characteristic," Ph.D. thesis, Academy of Machinery Science and Technology, Wuhan, China, 2008, unpublished.

[9] M.S. Plesset and R.B. Chapman, "Collapse of an initially spherical vapour cavity in the neighbourhood of a solid boundary," J. Fluid Mech, vol. 47, pp. 283-290, July 1971.

[10] C.F. Kennedy and J.E. Field, "Damage threshold velocities for liquid impact," J. Mater. Sci, vol. 35, pp. 5331-5339, February 2000.

[11] J. Luo, J. Li and G.N. Dong, "Two-dimensional simulation of the collapse of vapor bubbles near a wall," ASME J. Fluids Eng, vol. 130, pp. 1-4, August 2008.

[12] J. Li and H.S. Chen, "Numerical simulation of micro bubble collapse near solid wall in fluent environment," Tribology, vol. 28, pp. 311-315, July 2008, China.

[13] F. Burdin, N.A. Tsochatzidis, P. Guiraud, A.M. Wilhelm and H. Delmas, "Characterisation of the acoustic cavitation cloud by two laser techniques," Ultrason. Sonochem, vol. 6, pp. 43-51, March 1999.

[14] M. Dular, B. Stoffel and B. Širok, "Development of a cavitation erosion model," Wear, vol. 261, pp. 642-655, February 2006.

[15] T. Obara, N.K. Bourne and J.E. Field, "Liquid-jet impact on liquid and solid surfaces," Wear, vol. 186, pp. 388-394, 1995,.

[16] Y. Tomita and A. Shima, "Mechanisms of impulsive pressure generation and damage pit formation by bubble collapse," J. Fluid Mech, vol. 169, pp. 535-564, August 1986,.

[17] Z.C. Wang, Y. Zhang and X.Q. Zhang, "Thermal effect of cavitation erosion," Chinese J. Mater. Res, vol. 15, pp. 287-190, June 2001.

[18] Z.Y. Chen, "The role of oxidization in cavitation damage," J. Harbin Eng. Univ, vol. 28, pp. 1056-1059, September 2007.

[19] D. Bonamy, S. Prades, C.L. Rountree, L. Ponson, D. Dalmas, E. Bouchaud, K. Ravi-Chandar and C. Guillot, "Nanoscale damage during fracture in silica glass," Int. J. Fracture, vol. 140, pp. 3-14, January 2006.